Development/Plasticity/Repair

Transthyretin Internalization by Sensory Neurons Is Megalin Mediated and Necessary for Its Neuritogenic Activity

Carolina E. Fleming,[1,3] Fernando Milhazes Mar,[1] Filipa Franquinho,[1] Maria J. Saraiva,[1,2] and Mónica M. Sousa[1]

[1]Instituto de Biologia Molecular e Celular–IBMC, Nerve Regeneration Group and Molecular Neurobiology Group, 4150-180 Porto, Portugal, [2]Instituto de Ciências Biomédicas Abel Salazar, Universidade do Porto, 4099-003 Porto, Portugal, and [3]Programa Doutoral em Biologia Experimental e Biomedicina, Universidade de Coimbra, 3004-517 Coimbra, Portugal

Mutated transthyretin (TTR) causes familial amyloid polyneuropathy, a neurodegenerative disorder characterized by TTR deposition in the peripheral nervous system (PNS). The origin/reason for TTR deposition in the nerve is unknown. Here we demonstrate that both endogenous mouse TTR and TTR injected intravenously have access to the mouse sciatic nerve. We previously determined that in the absence of TTR, both neurite outgrowth *in vitro* and nerve regeneration *in vivo* were impaired. Reinforcing this finding, we now show that local TTR delivery to the crushed sciatic nerve rescues the regeneration phenotype of TTR knock-out (KO) mice. As the absence of TTR was unrelated to neuronal survival, we further evaluated the Schwann cell and inflammatory response to injury, as well as axonal retrograde transport, in the presence/absence of TTR. Only retrograde transport was impaired in TTR KO mice which, in addition to the neurite outgrowth impairment, might account for the decreased regeneration in this strain. Moreover, we show that *in vitro*, in dorsal root ganglia neurons, clathrin-dependent megalin-mediated TTR internalization is needed for TTR neuritogenic activity. Supporting this observation, we demonstrate that *in vivo*, decreased levels of megalin lead to decreased nerve regeneration and that megalin's action as a regeneration enhancer is dependent on TTR. In conclusion, our work unravels the mechanism of TTR action during nerve regeneration. Additionally, TTR presence in the nerve, as is here shown, may underlie its preferential deposition in the PNS of familial amyloid polyneuropathy patients.

Introduction

When mutated, transthyretin (TTR) is related to familial amyloid polyneuropathy (FAP) (Saraiva 2001), a neurodegenerative disorder characterized by extracellular deposition of TTR aggregates and amyloid fibrils, particularly in the peripheral nervous system (PNS) (Andrade, 1952). As a consequence of TTR deposition, axonal degeneration arises, ending up in neuronal loss. Several clues have emerged as to the molecular mechanisms of TTR-mediated cellular toxicity leading to neurodegeneration in FAP (Sousa and Saraiva, 2003). The origin of TTR deposited in the PNS of FAP patients is however unknown. TTR is mainly synthesized by the liver and the choroid plexus that are respectively the sources of TTR in the plasma and CSF. TTR was reported as being expressed in the PNS, namely by glial cells of dorsal root ganglia (DRG) (Murakami et al., 2008). However, this issue was clarified in a subsequent study showing that TTR synthesis does not occur in DRG cells (Sousa and Saraiva, 2008). Under physiological conditions serum-free human and rat nerve endoneurial fluid display TTR immunoreaction (Saraiva et al., 1988). TTR may have access to the nerve through the blood-nerve barrier (BNB), and/or through contact between peripheral nerve roots and CSF, where TTR is present in high levels. In fact, in recipients of FAP livers, i.e., after domino liver transplantation, TTR deposits are found within the nerve of the recipients, suggesting that plasma TTR (synthesized in the liver) can cross the BNB (M. M. Sousa et al., 2004).

Apart from being a transporter of thyroxine (T_4) and retinol, TTR has been described as having functions related to the nervous system, namely to be involved in cognition (Brouillette and Quirion, 2008), behavior (J. C. Sousa et al., 2004), and neuropeptide processing (Nunes et al., 2006). In the case of the PNS, it was demonstrated that TTR enhances peripheral nerve regeneration (Fleming et al., 2007). In that study, TTR knock-out (KO) mice presented delayed functional and morphological recovery after nerve injury, as assessed from a decreased number of myelinated and unmyelinated axons in the course of regeneration. TTR capacity to enhance nerve regeneration was unrelated to neuronal survival as the absence of TTR was not accompanied by increased neuronal loss. In transgenic mice expressing human TTR in neurons, in a TTR KO background, the delayed regeneration of TTR KO mice was rescued, reinforcing that TTR enhances nerve regeneration (Fleming et al., 2007). Additionally, absence of TTR was found to be related to a decreased ability of DRG neurons to

Received Dec. 18, 2008; revised Feb. 5, 2009; accepted Feb. 10, 2009.

This work was supported by Association Française contre les Myopathies (AFM), France, and Fundação para a Ciência e a Tecnologia (FCT), Portugal (Grants PTDC/BIA-PRO/64437/2006 and SAU-OSM/64093/2006). C.E.F. was the recipient of a Programa Doutoral em Biologia Experimental e Biomedicina fellowship (SFRH/BD/9682/2002) from Centro de Neurosciências de Coimbra/FCT (POCI 2010, FSE), Portugal, and of an AFM fellowship (AM/NM/2006.1272/FN12047). F.M.M. is the recipient of an FCT fellowship (SFRH/BD/43484/2008). We thank Rui Fernandes and Vera Sousa [Instituto de Biologia Molecular e Celular (IBMC)] for tissue processing and electron microscopy, Dr. Paula Sampaio (IBMC) for help in confocal microscopy, Dr. Rosário Almeida (IBMC) for help in T_4 binding assays, Dr. Márcia Liz (IBMC) for the production of TTR, and Dr. Pedro Brites (AMC, Amsterdam) for critical reading of this manuscript.

Correspondence should be addressed to Mónica M. Sousa, Nerve Regeneration Group, Instituto de Biologia Molecular e Celular–IBMC, R. Campo Alegre 823, 4150-180 Porto, Portugal. E-mail: msousa@ibmc.up.pt.

DOI:10.1523/JNEUROSCI.6012-08.2009

 0270-6474/09/293220-13$15.00/0

grow neurites *in vitro*: cells grown without TTR displayed a reduced number of neurites, as well as a decreased size of the longest neurite (Fleming et al., 2007). This TTR neuritogenic effect was demonstrated to be independent of its major ligands, retinol and T_4. The newly described TTR role in peripheral nerve biology might explain why, when mutated, the protein preferentially accumulates in the PNS. Yet, the means through which TTR increases regeneration is unknown.

In the current work, we aimed at finding the mechanism through which TTR enhances nerve regeneration and neurite outgrowth.

Materials and Methods

Mice. Mice were handled according to European Union and National rules. WT and TTR KO (Episkopou et al., 1993) littermates (in the 129/Sv background), as well as megalin heterozygous [MEG (+/−), kindly provided by Dr. Thomas Willnow, Max-Delbrueck Center for Molecular Medicine, Berlin, Germany] and TTR KO/MEG (+/−) littermate mice (in the 129/Sv background), were obtained from the offspring of heterozygous breeding pairs. All animals were maintained under a 12 h light/dark cycle and fed with regular rodent's chow and tap water *ad libitum*. Genotypes were determined from tail extracted genomic DNA. Unless otherwise stated, all comparisons comprised groups of 6 animals per genotype, age- and sex-matched. For TTR detection in the nerve and nerve injury experiments, either 3 or 6 months old animals were used. For DRG neuron cultures, animals with 1–4 weeks of age were used. All experiments were performed with the observer blinded to the animal's genotype.

Nerve injury. Mice were anesthetized with medetomidine/ketamine and a 4-mm-long incision was made in the shaved thigh skin. For nerve crush, the sciatic nerve was exposed and crush was performed using Pean forceps, twice during 15 s. To standardize the procedure, the crush site was maintained constant for each animal at 35 mm from the tip of the third digit. A single skin suture, immediately above the crush site, served as an additional reference. After surgery, animals were allowed to recover for 5, 15, 30, or 75 d. For chronic constriction injury (CCI), the sciatic nerve was exposed and one ligature was tied around the nerve using 4/0 silk suture material (Braun). Skin was sutured and mice were allowed to recover for 24 h. Mice were perfused for 20 min with PBS through the vena cava at a flow rate of 2 ml/min and the sciatic nerve was subsequently collected.

Assessment of mouse TTR presence in the nerve after nerve crush. WT mice underwent nerve crush and were allowed to recover for 3 d. Mice were perfused for 20 min with PBS through the vena cava at a flow rate of 2 ml/min and the distal nerve segments were subsequently collected. Western blot was performed as described below. The primary antibody used was a custom made rabbit anti-mouse TTR antibody (produced against recombinant mouse TTR, 1:500). Electronic microscopy using WT distal nerve segments was performed as described below.

Assessment of TTR access to the nerve. TTR was produced as previously described (Liz et al., 2004), and 1 mg of recombinant human TTR was conjugated with Alexa 488 using the Alexa Fluor 488 labeling kit (Invitrogen), according to the manufacturer's instructions. hTTR-Alexa 488 was separated from free Alexa 488 by fine size exclusion chromatography in Bio-Rad BioGel P-30 resin columns. Subsequently, 1 μg of hTTR-Alexa 488 was run in a 15% SDS polyacrylamide gel and, after electrophoresis, hTTR-Alexa 488 was visualized in a Typhoon 8600 (Amersham) to check labeling efficacy. hTTR-Alexa 488 (100 μg) was injected intravenously in the tail vein of WT and TTR KO mice. The next day, mice were subjected to unilateral nerve crush as described above. The following day, mice were killed, and both crushed and contralateral sciatic nerves were collected and cryoprotected with a 1.2% L-lysine solution containing 2% formalin. For immunohistochemistry using the primary rabbit anti-human TTR (Dako; 1:1500), and rabbit anti-mouse TTR (1:2000) polyclonal antibodies, 10 μm-thick sections were incubated in 0.1% sodium borohydride (Sigma) for 5 min. Sections were then blocked in blocking buffer (1% bovine serum albumin and 4% fetal bovine serum in PBS) for 1 h at room temperature, and incubated with primary antibody diluted in blocking buffer overnight. As a negative control, slides were left overnight at 4°C with either anti-mouse (TTR previously adsorbed with recombinant mouse TTR, produced as previously described (Liz et al., 2004), or with blocking buffer alone. The adsorption of anti-mouse TTR was performed by incubation of 200 μg of recombinant mouse TTR with 1 μl of anti-mouse TTR overnight at room temperature with agitation. After centrifugation at 16,000 g, the supernatant, diluted 1:2000 in blocking buffer, was used to perform immunohistochemistry. Subsequently, slide incubation with the anti-rabbit IgG-Alexa 568 secondary antibody (Invitrogen, 1:1000) diluted in blocking buffer was performed for 1 h at room temperature. Coverslips were mounted with VectaShield Mounting Medium with DAPI (Vector), and images were taken using a Leica SP2 AOBS SE (Leica) confocal laser scanning microscope.

Local delivery of TTR to the crushed nerve. WT and TTR KO mice underwent bilateral nerve crush as described above. Immediately after crush and before suturing, 80 μl of Matrigel Basement Membrane Matrix (BD Biosciences) was applied to the left sciatic nerve crush site; the right sciatic nerve crush site received 80 μl of Matrigel Basement Membrane Matrix supplemented with 60 μg of recombinant WT TTR, produced as previously described (Liz et al., 2004). Ten minutes after Matrigel application, when it had already gelled, skin was sutured. The animals were allowed to recover for either 15 or 30 d. Mice were killed using a lethal anesthesia dosage, and the left and right nerve distal stumps were collected and processed for morphometric analysis as described below. To assess for the presence of TTR in the nerve after Matrigel application, similar experiments were performed where 80 μl of Matrigel supplemented with 60 μg of hTTR-Alexa 488 (produced as described above) were applied to the right sciatic nerve crush site of TTR KO mice; to the left sciatic nerve crush site, Matrigel supplemented with free Alexa 488 (equivalent to the amount of fluorophore present in 60 μg of hTTR-Alexa 488) was applied. As an additional negative control, a group of animals received Matrigel alone in the sciatic nerve crush site. Mice were killed 1 d after Matrigel application and the nerve (3–4 mm upstream and downstream of the crush site) was collected, cryoprotected with a 1.2% L-lysine solution containing 2% formalin and sectioned at 8 μm. The presence of hTTR-Alexa 488 was detected using a using a Leica SP2 AOBS SE (Leica Microsystems) confocal laser scanning microscope.

Morphometric analysis. The 3 mm segments immediately distal to the crush site were fixed overnight in 1.25% glutaraldehyde in 0.1 M sodium cacodylate, washed in 0.1 M sodium cacodylate for 30 min, postfixed in 1% osmium tetroxide in 0.2 M sodium cacodylate for 60 min, washed again in 0.1 M sodium cacodylate for 30 min, dehydrated using a series of graded alcohols and propylene oxide, and embedded in epon. Transverse sections (1.0 μm thick) were cut with a SuperNova, Reichest, Leica ultramicrotome, and stained with 1% toluidine blue in an 80°C heating plate for 20 s. For each animal, the total number of myelinated fibers present in one semithin section was determined by counting 50× magnified photographs covering the whole nerve area. To determine the density of unmyelinated fibers, ultrathin transverse sections were cut and stained with uranyl acetate and lead citrate. For each animal, 20 nonoverlapping photomicrographs (7000× amplification) corresponding to ~9000 μm^2 of each ultrathin section were taken using a transmission electron microscope (Zeiss 10C) and analyzed. To assess possible differences in nerve total areas between strains, these were determined from 10× magnified photos of sciatic nerve transverse sections.

Analysis of Schwann cell proliferation. WT and TTR KO mice underwent bilateral nerve crush and were allowed to recover for 5 d. To label dividing cells, 100 μg/g body weight of BrdU (5-bromo-2′-deoxyuridine, Sigma) was injected intraperitoneally 4 and 2 h before kill. Labeling of proliferating cells was performed 5 d after injury, since at this time point, Schwann cells reach their maximum proliferative activity in injured sciatic nerves (Cheng and Zochodne, 2002). Mice were killed using a lethal anesthesia dosage and the sciatic nerves were collected and processed for immunohistochemistry. Nerves were excised, fixed in 4% neutral buffered formalin and embedded in paraffin. Sections (5 μm thick) were deparafinated in histoclear (National Diagnostics) and hydrated in a descendent alcohol series. Antigen unmasking was done by incubation in 2N HCl for 20 min at 37°C, followed by neutralization with 0.1 M $Na_2B_4O_7$, and incubation with trypsin-EDTA (Invitrogen) for 10 min at

37°C. Immunohistochemistry using the primary anti-BrdU monoclonal antibody (1:1000, Sigma) was performed with the MOM kit (Vector) according to the manufacturer's instructions, using diaminobenzidine (Sigma) as substrate. Slides were counterstained with hematoxylin (Merck). Two longitudinal nerve sections per animal were immunostained; four 50× magnified photographs per section distal to the crush site were taken, covering an area of ~0.5 mm^2, and the number of BrdU-labeled nucleus was determined, as well as the total number of nucleus stained with hematoxilin. The percentage of BrdU-labeled nucleus was then calculated for each animal.

Assessment of apoptosis by TUNEL analysis. The comparison of apoptotic cells in crushed nerves from WT and TTR KO mice was performed with the ApopTag Peroxidase *In Situ* Apoptosis Detection Kit (Millipore Bioscience Research Reagents), according to the manufacturer's instructions, using diaminobenzidine (Sigma) as substrate. Slides were counterstained with hematoxylin (Merck). Eight 10× magnified photographs per section near the crush site were taken, covering an area of ~0.15 mm^2. For each animal, the number of labeled nucleus was determined, as well as the total number of nucleus stained with hematoxilin. The percentage of apoptotic nucleus was then calculated for each animal.

Determination of macrophage number. Semithin sections stained with toluidine blue of WT and TTR KO sciatic nerve distal segments were obtained as described above for morphometric analysis. For each animal, the density of macrophages present in one semithin section covering the whole nerve area was determined by observation of 20× magnified photographs 15, 30, and 75 d after nerve crush.

Western blot. Intact and CCI nerves were sonicated in 0.5% Triton X-100 (Sigma) containing protease inhibitor mix (Amersham). Protein (12 μg total per lane) was run in 15% SDS polyacrylamide gels. After electrophoresis, samples were transferred to a nitrocellulose membrane (Amersham), blocked with blocking buffer (5% nonfat dried milk in PBS), and incubated overnight at 4°C with primary antibodies diluted in blocking buffer, namely, rabbit polyclonal anti-$p75^{NTR}$ (Santa Cruz Biotechnology, 1:200), and mouse monoclonal anti-β-actin (Sigma; 1:5000). Subsequently, incubation with horseradish peroxidase (HRP)-labeled secondary antibodies diluted in blocking buffer, namely either anti-rabbit IgG-HRP (The Binding Site; 1:10,000) or anti-mouse IgG-HRP (The Binding Site; 1:5000), was performed for 1 h at room temperature. Blots were developed using the ECL PlusTM Western blotting reagents (Amersham) and exposed to Hyperfilm ECL (Amersham). Quantitative analysis of Western blots was performed using the ImageQuant software (Amersham). Results are shown as the ratio between $p75^{NTR}$ and β-actin signals.

Primary cultures of DRG neurons. Primary cultures of DRG neurons were performed as described previously (Lindsay, 1988). Briefly, DRG were dissected aseptically from WT or TTR KO mice, freed of roots and treated with 0.125% collagenase (Sigma) for 3 h at 37°C. After enzyme treatment, a single-cell suspension was obtained by trituration with a fire-polished Pasteur pipette. The cell suspension was centrifuged into a 15% albumin gradient for 10 min at 200 g. The obtained pellet was resuspended in Neurobasal medium supplemented with B27, penicillin-streptomicin, glutamine, fungizone (all from Invitrogen) and 50 ng/ml NGF (Sigma), plated in poly-L-lysine coated 13 mm coverslips and maintained at 37°C.

Transferrin transport assay. The use of human transferrin conjugated with Texas red (Tf-TR, Invitrogen) as a tracer to examine retrograde transport in cultures of DRG neurons has been previously documented (Liu et al., 2003). WT and TTR KO DRG neurons were cultivated as described above. After 3 d in culture, cells were incubated with medium containing 50 μg/ml Tf-TR for 2 h at 37°C to allow uptake. Cells were then washed and incubated with Neurobasal medium supplemented with B27, penicillin-streptomicin, glutamine, fungizone (all from Invitrogen), and 50 ng/ml NGF (Sigma). Twenty-seven hours later, neurons were fixed in 2% neutral buffered formalin for 30 min, washed with PBS, and kept at 4°C until use. Slides were mounted in VectaShield Mounting Medium with DAPI (Vector). Images were taken using a Leica SP2 AOBS SE (Leica Microsystems) confocal laser-scanning microscope. For the quantification of Tf-TR labeling in DRG neurons, a semiquantitative scale ranging from 1 to 5 was used as follows: 1, Tf-TR present in 100% of the neurites; 2, Tf-TR present in >50% of the neurites; 3, Tf-TR present in 50% of the neurites; 4, Tf-TR present in <50% of the neurites; 5, Tf-TR absent from neurites (i.e., only present in the cell body).

In vivo *analysis of retrograde transport using cholera toxin B.* The sciatic nerve of WT and TTR KO mice was exposed and transected at the midtight level; a solution of the retrogradely transported cholera toxin B subunit (0.5 mg/ml, List Biological) was applied to the proximal end of the transected sciatic nerve for 35 min. The skin was subsequently sutured and mice were allowed to recover for 72 h, after which the L4–6 DRG were collected and fixed in 4% neutral buffered formalin. To detect retrogradely labeled sensory neurons, serial 4-μm-thick DRG sections were cut and processed for anti-cholera toxin immunohistochemistry. Briefly, sections were blocked in blocking buffer (1% bovine serum albumin and 4% fetal bovine serum in PBS) for 30 min at 37°C and incubated with anti-cholera toxin antibody (Calbiochem; 1:1000) diluted in blocking buffer overnight at 4°C. Antigen visualization was performed with the biotin-extravidin-peroxidase kit (Sigma). For each animal, to determine the percentage of retrogradely labeled sensory neurons, the total number of DRG neurons, as well as the number of labeled DRG neurons presenting visible nuclei, were counted every 24 μm.

Analysis of TTR endocytosis by DRG neuron cultures. Primary cultures of DRG neurons were performed as described above (Lindsay, 1988). Cells were maintained for 96 h at 37°C. After this period, DRG neurons were supplemented with 300 μg/ml recombinant human TTR conjugated with Alexa 488 (hTTR-Alexa 488, produced as described above) for 3 h at 4°C or 37°C. When mentioned, neuronal cells were additionally incubated with 50 μg/ml transferrin conjugated with Texas red (Tf-TR, Invitrogen) or with 5 μg/ml cholera toxin subunit B conjugated with Alexa Fluor 647 (CT-B, Invitrogen). Cells were fixed in 2% neutral buffered formalin for 30 min, washed with PBS and kept at 4°C until immunostaining. For immunocytochemistry, DRG neurons were permeabilized with 0.2% Triton X-100 (Sigma) and were then incubated with 0.1% sodium borohydride (Sigma). For immunocytochemistry using the primary antibody rabbit anti-PGP 9.5 (1:500, Ab Serotec), coverslips were blocked in MOM IgG Blocking reagent (Vector) for 1 h at room temperature, and incubated with primary antibody diluted in MOM diluent (Vector) overnight at 4°C. Subsequently, incubation with the secondary antibody anti-rabbit IgG-Alexa 568 (1:1000, Invitrogen) diluted in MOM diluent was performed for 1 h at room temperature. Coverslips were mounted with VectaShield Mounting Medium containing DAPI (Vector), and images were taken using a Leica SP2 AOBS SE (Leica Microsystems) confocal laser scanning microscope.

Analysis of TTR endocytosis by transfected DRG neurons. Primary DRG neurons were obtained as already detailed. After DRG neuron isolation and prior plating, ~250,000 neurons were transfected with 10 μg of GFP-tagged Eps15 constructs (a kind gift from Dr. Benmerah, Institut Cochin, Paris, France), isolated using the Endofree Plasmid Maxi kit (Qiagen, Portugal). Transfection was performed in a Amaxa Nucleofector (Amaxa Biosystems), using program A-033 and the Mouse Neuron Nucleofector kit (Amaxa Biosystems). Transfected cells were subsequently plated in 24-well plates at a density of ~30,000 cells/well. Cells were maintained for 48 h at 37°C after which they were supplemented with 300 μg/ml recombinant human TTR conjugated with Alexa 568 (hTTR-Alexa 568, produced similarly as described above for hTTR-Alexa 488) for 3 h at 37°C. Cells were then processed for PGP 9.5 immunocytochemistry, as described above, using as secondary antibody anti-rabbit IgG-Alexa 647 (1:1000, Invitrogen). For quantification of hTTR-Alexa 568 internalization, images of randomly selected PGP 9.5 labeled cells were taken along the *z*-axis in a Leica SP2 AOBS SE confocal laser scanning microscope, using the same laser intensity for all conditions. hTTR-Alexa 568 internalization in cells photographed in each of the conditions was then determined using the ImageJ software (http://rsbweb.nih.gov/ij/) and calculated as total brightness intensity in the 568 channel (expressed as arbitrary units)/cell.

Measurement of neurite outgrowth using TTR coupled to FluoSpheres. Recombinant WT TTR (2 mg) was covalently bound to 1 μm-diameter carboxylate- or amine-modified FluoSpheres (Invitrogen), using a carbodiimide cross-linking method, according to the manufacturer's instructions. FluoSpheres bound to TTR were washed three times with PBS

and the efficacy of the method was evaluated by running the three washes containing free uncoupled WT TTR in a 15% SDS polyacrylamide gel; >90% of WT TTR was bound to the FluoSpheres and no detectable free TTR was found within the last wash. PC12 cells (European Collection of Cell Cultures), a rat adrenal cell line with a neuronal-like phenotype, were grown in six-well plates in DMEM (Invitrogen) supplemented with 10% fetal bovine serum (Invitrogen). When cells reached 50% confluence, fetal bovine serum was withdrawn and cells were supplemented with either: (1) 10% of either WT or TTR KO mouse serum, (2) 10% TTR KO mouse serum containing 300 μg/ml recombinant WT TTR, (3) 10% of TTR KO mouse serum containing 0.12% of free FluoSpheres, (4) 10% of TTR KO mouse serum containing 300 μg/ml free recombinant WT TTR and 0.12% of free FluoSpheres, and (5) 10% of TTR KO mouse serum containing 300 μg/ml recombinant WT TTR coupled to 0.12% FluoSpheres. Fifty hours later, PC12 cells were fixed in 2% neutral buffered formalin for 30 min, washed with PBS and kept at 4°C until further analysis. Neurite size was determined from 50× magnified fields. At least 150 cells were analyzed for each condition. To check whether TTR was biologically active when coupled to FluoSpheres, its ability to bind T_4 was evaluated. Briefly, a 100 μl suspension of either free FluoSpheres (0.12%) or 8.25 μg/ml TTR coupled to FluoSpheres (0.12%) was incubated with 50,000 cpm of [^{125}I]T_4 (Perkin-Elmer) in triplicates overnight at 4°C. As an internal control to ascertain the specificity of T_4 binding to TTR, 100 μl suspension of the same samples were coincubated with 50,000 cpm of [^{125}I]T_4 and nonradioactive T_4 in molar excess. Subsequently, FluoSpheres were washed three times with PBS and radioactivity of the pellets, corresponding to T_4 bound to TTR, was counted in a gamma-spectrometer (Wallac).

Analysis of TTR endocytosis in DRG neurons blocked with sheep anti-rat megalin antibody. After DRG neuron isolation, cells were plated in 24-well plates at a density of ~10,000 cells/well. Cells were maintained for 96 h at 37°C after which they were preincubated for 2 h at 37°C with sheep anti-rat megalin (1:200, kindly provided by Dr. Pierre Verroust, CHU Saint Antoine, Paris, France) or nonimmune sheep serum (using an equal volume as the one used in the case of sheep anti-rat megalin). Subsequently, DRG neurons were supplemented with 300 μg/ml hTTR-Alexa 488 in the presence of sheep anti-rat megalin or nonimmune sheep serum (in the same conditions as used for the preincubation) for 3 h at 37°C. It is noteworthy that this anti-megalin antibody has been used previously to successfully inhibit megalin-dependent internalization (Klassen et al., 2004). DRG neurons were then processed for PGP 9.5 immunocytochemistry as described above using as secondary antibody anti-rabbit IgG-Alexa 568 (1:1000, Invitrogen). For quantification of hTTR-Alexa 488 internalization, images of randomly selected PGP 9.5 labeled cells were taken along the *z*-axis in a Leica SP2 AOBS SE confocal laser scanning microscope, using the same laser intensity for all conditions. The intensity of internalized hTTR-Alexa 488 in DRG neurons treated with either sheep anti-rat megalin or nonimmune sheep serum was then determined using the ImageJ software (http://rsbweb.nih.gov/ij/), as described above.

Measurement of neurite outgrowth in the presence of TTR and anti-rat megalin. TTR KO DRG neurons were maintained for 48 h at 37°C, after which DRG neurons were supplemented with (1) B27 or B27 containing either (2) 300 μg/ml recombinant TTR, (3) 300 μg/ml recombinant TTR and 200 μg/ml sheep anti-rat megalin (kindly provided by Dr. Pierre Verroust), (4) 200 μg/ml sheep anti-rat megalin, and (5) 300 μg/ml recombinant TTR and 200 μg/ml IgG (IgG, Sigma). As an additional control, in an independent experiment, DRG neurons were supplemented with B27 containing a volume of nonimmune sheep serum equal to the one of sheep anti-rat megalin used in condition (5). Fifty hours later, cells were fixed in 2% neutral buffered formalin for 30 min, washed with PBS and kept at 4°C until further analysis. Neurite size was determined from 50× magnified fields. At least 180 cells were analyzed for each condition.

Megalin immunohistochemistry and RT-PCR. For RT-PCR, total RNA from mouse DRG and kidney was isolated using Trizol (Invitrogen). cDNA was obtained using the Superscript II kit (Invitrogen). PCR was performed using the following sense and antisense primers: for mouse megalin, 5′-CCTTGCCAAACCCTCTGAAAAT-3′ and 5′-CACAAGGTTTGCGGTGTCTTTA-3′ and for mouse HPRT, 5′-GTAATGATCAGTCAACGGGGGAC-3′ and 5′-CCAGCAAGCTTGCAACCTTAACCA-3′. Ethidium bromide-stained gels were scanned using a Typhoon 8600 (Amersham). For immunohistochemistry using the sheep anti-megalin primary antibody (1:2000, kindly provided by Dr. Pierre Verroust), antigen unmasking was done by boiling 3× in 0.5 mM EDTA 10 mM Tris pH = 9.0 solution. Sections were blocked in blocking buffer (1% bovine serum albumin and 4% fetal bovine serum in PBS) for 30 min at 37°C and incubated with primary antibody diluted in blocking buffer overnight at 4°C. Antigen visualization was performed with the biotin-extravidin-peroxidase kit (Sigma). Slides were counterstained with hematoxylin (Merck).

Statistical analysis. Statistical analysis was performed using the Student's *t* test. Results were expressed as average ± SEM.

Results

TTR is detectable within the endoneurium of both control and crushed nerves

We recently determined that TTR enhances nerve regeneration (Fleming et al., 2007). Upon nerve injury, disruption of the BNB occurs, leading to the exposure of the nerve to plasma proteins. To verify the disruption of the BNB by nerve crush, ultrathin nerve sections were analyzed, 3 d after crush; blood residues were observed near the crush site (Fig. 1*A*). To check whether TTR was present in the nerve 3 d after crush, mouse TTR immunoblotting of crushed nerves from perfused WT mice was performed. As illustrated in Figure 1*B*, TTR is indeed present in the nerve after crush, in the course of regeneration. As positive and negative controls, CSF from WT mice (WT CSF) and nerve extracts from TTR KO mice (TTR KO nerve) were used, respectively (Fig. 1*B*).

To further unveil the presence of TTR in the nerve in the settings of nerve injury, we performed immunohistochemistry against mouse TTR (mTTR) in crushed nerves from WT mice. mTTR was readily detected within the nerve, along nerve fibers (Fig. 1*Ca*). To confirm the specificity of mTTR immunohistochemistry, three different negative controls were performed: mTTR immunohistochemistry of (1) TTR KO crushed nerves (Fig. 1*Cb*), (2) WT crushed nerves using the anti-mTTR primary antibody previously adsorbed with recombinant mTTR (Fig. 1*Cc*), and (3) WT crushed nerves in the absence of primary antibody (Fig. 1*Cd*). As expected, no reactivity was present in the negative controls. Considering the prompt detection of TTR in the crushed nerve, we followed by investigating whether TTR was detectable in the nerve under physiological conditions. mTTR immunohistochemistry of WT intact nerves revealed that TTR is readily detectable in the nerve (Fig. 1*Da*) with a similar immunostaining pattern as the one observed after nerve crush (Fig. 1*Ca*). The analysis of transverse sections of WT intact nerves stained for mTTR suggests that TTR is probably present in the extracellular matrix surrounding nerve fibers, as visualized by colocalization with brightfield images (Fig. 1*Db–d*).

To further understand how TTR gains access to the nerve after injury, hTTR-Alexa 488 was injected intravenously 1 d before nerve crush; 1 d after crush, nerves were collected and cryopreserved. Subsequently, crushed nerves were screened for green fluorescence. Interestingly, hTTR-Alexa 488 was found within the nerve, along fibers (Fig. 1*Eb*). The same pattern was found in WT and TTR KO nerves (data not shown). To verify that the green fluorescence corresponded to injected hTTR-Alexa 488, immunohistochemistry against human TTR (hTTR) was performed, showing that both signals colocalized (Fig. 1*Eb–d*), confirming that plasma TTR enters the sciatic nerve after crush.

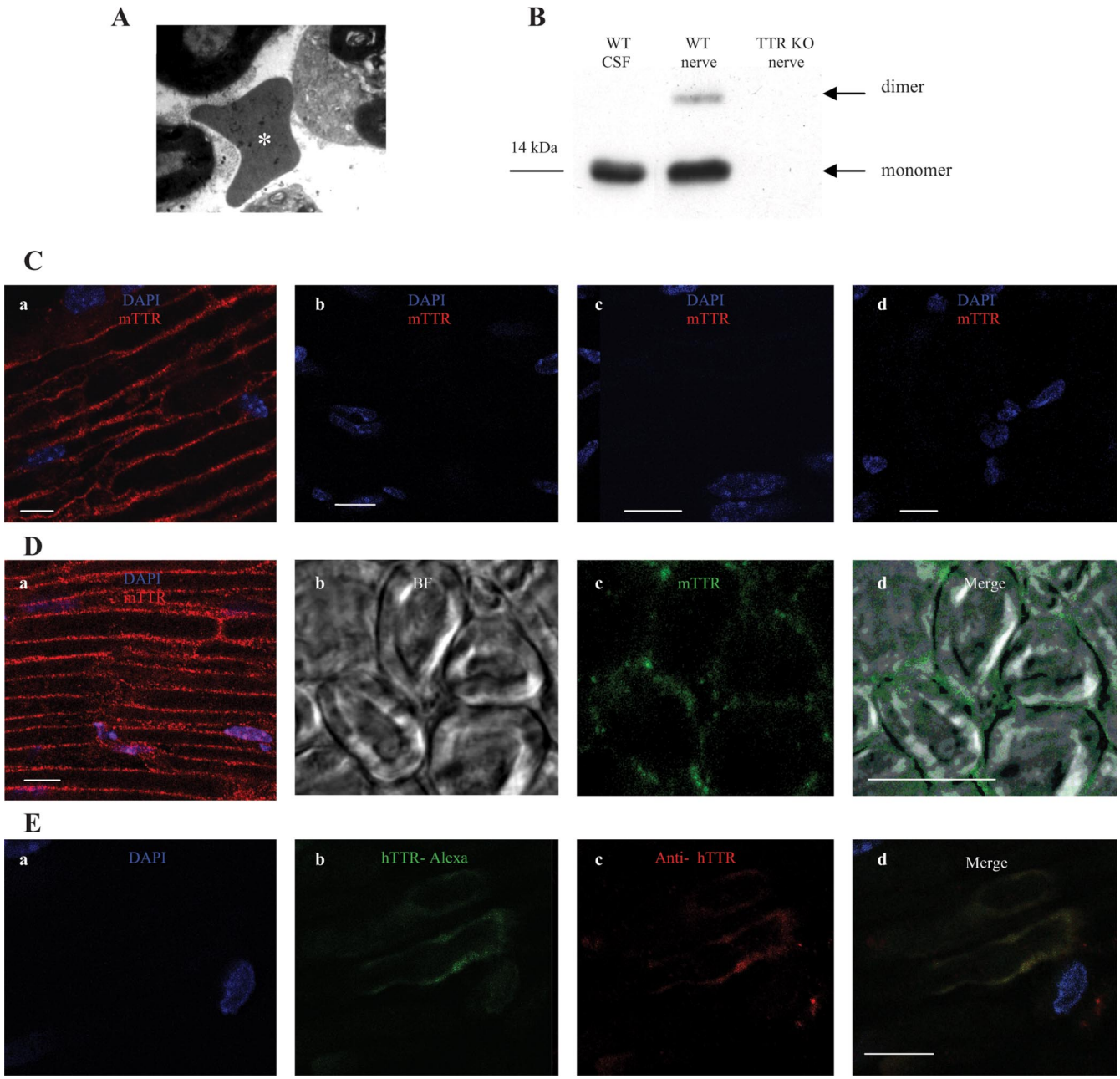

Figure 1. TTR presence in the nerve. ***A***, ***B***, TTR presence in the nerve 3 d after nerve crush as assessed by evaluation of ultrathin sections from a WT sciatic nerve near the crush site (asterisk highlights blood accumulation) (***A***), and anti-mouse TTR Western blot of WT mouse CSF (WT CSF), crushed nerves from WT (WT nerve), and TTR KO mice (TTR KO nerve) (TTR monomer and dimer are indicated by arrows) (***B***). ***C***, mTTR presence in the nerve after injury detected by immunohistochemistry in WT crushed nerves (***a***), TTR KO crushed nerves (***b***), and WT crushed nerves using anti-mTTR preincubated with recombinant mTTR (***c***), and in the absence of primary antibody (***d***); scale bars, 10 μm. ***D***, mTTR presence in intact nerves: (***a***) mTTR immunohistochemistry in a longitudinal section of an intact WT nerve and (***b–d***) mTTR immunohistochemistry of a transverse section of an intact WT nerve. BF, Brightfield. Scale bar, 10 μm. ***E***, Intravenously injected hTTR-Alexa 488 was found within WT crushed nerves along fibers: (***a***) DAPI immunostaining in blue, (***b***) hTTR-Alexa 488 in green, (***c***) hTTR immunostaining in red, and (***d***) merged image. Scale bar, 10 μm.

Local TTR delivery to the crushed nerve rescues the regeneration phenotype of TTR KO mice

In TTR KO mice, nerve regeneration is impaired: after 15 d of regeneration, the number of myelinated fibers is ~20% lower, whereas 30 d after injury, the density of unmyelinated fibers is ~40% decreased in this strain (Fleming et al., 2007). This impairment is recovered when TTR KO mice are backcrossed to mice expressing human TTR in neurons (Fleming et al., 2007). To determine if additionally, local TTR delivery to the injury site is sufficient to rescue the TTR KO phenotype, TTR was locally administrated to the crush site and mice were allowed to recover for either 15 or 30 d. Matrigel, the chosen vehicle, although containing other extracellular matrix components such as growth factors, is mainly constituted by laminin, that enhances nerve regeneration per se (Madison et al., 1985). To verify whether TTR released from Matrigel could be found at the nerve crush site, Matrigel supplemented with hTTR-Alexa 488 was initially used. As is shown in Figure 2*A*, hTTR-Alexa 488 could readily be found in the nerve crush site 1 d after Matrigel application (left); in nerves where free Alexa 488 was applied, no labeling was found, as expected (Fig. 2*A*, right).

Fifteen days after injury, the addition of Matrigel per se was

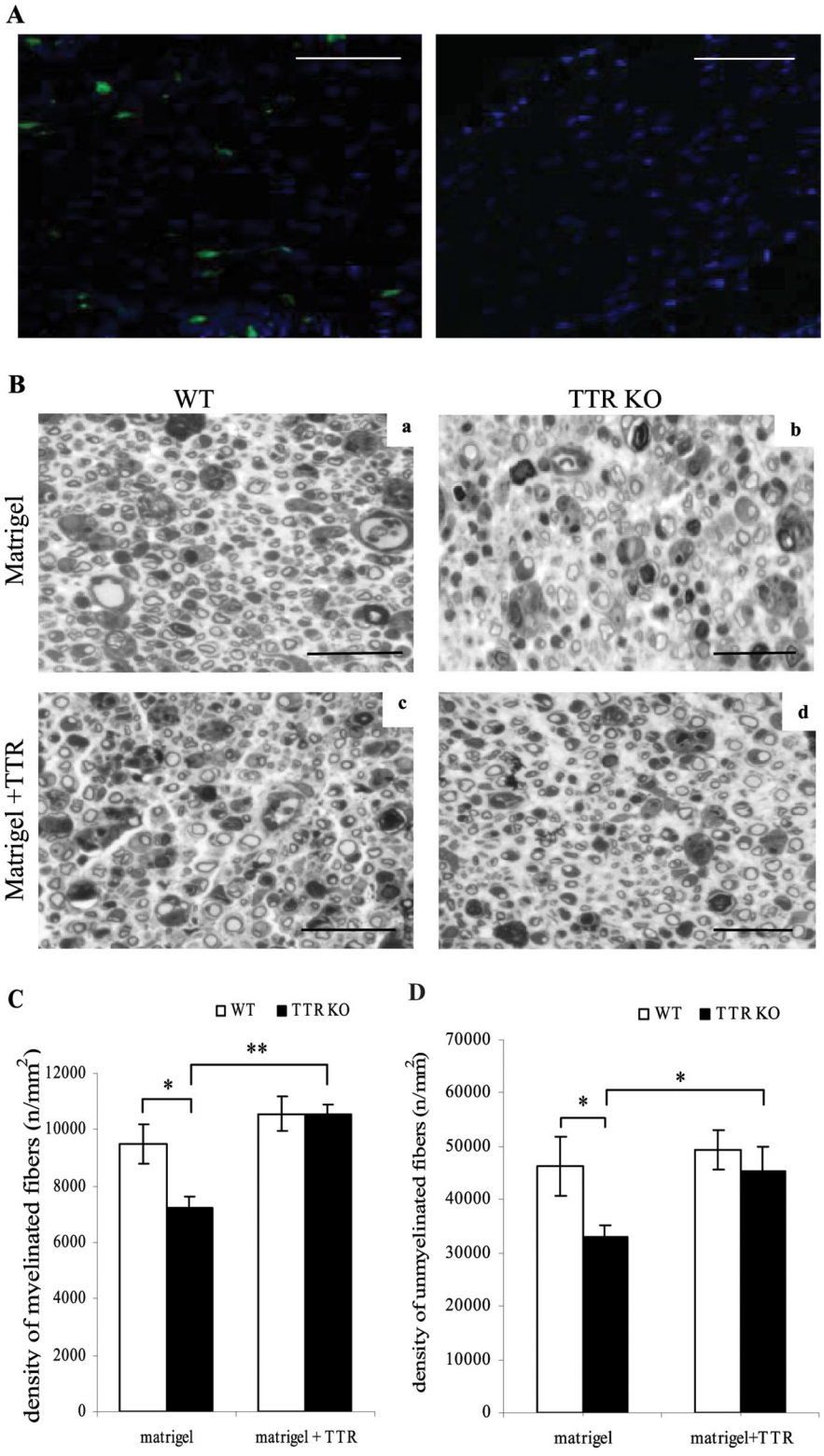

Figure 2. Local delivery of TTR to the crushed nerve. ***A***, Detection of green fluorescence in the sciatic nerve crush site 1 d after delivery of hTTR-Alexa 488 (left) or free Alexa 488 (right) in Matrigel. Scale bars, 100 μm; DAPI in blue. ***B***, Semithin sections of distal nerve stumps 15 d after nerve crush from WT mice (***a***, ***c***) and TTR KO mice (***b***, ***d***), in which Matrigel either alone (***a***, ***b***) or supplemented with TTR (***c***, ***d***) was added. Scale bars, 10 μm. ***C***, Corresponding density of myelinated fibers. WT: $n = 6$ and $n = 7$; TTR KO: $n = 5$ and $n = 7$, respectively, for each setting. ***D***, Density of unmyelinated fibers 30 d after nerve crush in WT and TTR KO mice, in which Matrigel either alone or supplemented with TTR was added. WT: $n = 6$ and $n = 5$; TTR KO: $n = 8$ and $n = 8$, respectively, for each setting; Matrigel alone (matrigel), Matrigel supplemented with TTR (matrigel+TTR). *$p < 0.05$, **$p < 0.01$.

not able to overcome the effect of lack of TTR, as TTR KO mice presented a 24% decreased density of myelinated fibers when compared with WT littermates (Fig. 2*B*,*C*). However, the addition of TTR to Matrigel was sufficient to rescue the regeneration delay of TTR KO mice, as their density of myelinated fibers reached WT levels (Fig. 2*B*,*C*).

Regarding unmyelinated fibers, at 15 d of regeneration no differences were found between the two strains (data not shown) which is in agreement with what was previously described at this time point after crush (Fleming et al., 2007). To further address whether TTR delivery to crushed nerves of WT and TTR KO mice could rescue the regeneration of unmyelinated fibers, their density was determined 30 d after injury. Similarly to what was observed for myelinated fibers, the addition of Matrigel per se was not able to overcome the lack of TTR, as 30 d after injury TTR KO mice presented a 30% decreased density of unmyelinated fibers when compared with WT littermates (Fig. 2*D*). However, the addition of TTR to Matrigel was able to rescue the regeneration impairment of TTR KO mice, as their density of unmyelinated fibers reached WT levels (Fig. 2*D*).

In TTR KO mice, after nerve crush, the Schwann cell response is unaffected while the inflammatory response reflects their delayed regeneration

Given that no effect of TTR on neuronal survival was found after nerve crush (Fleming et al., 2007), we assessed whether the delayed regeneration of TTR KO mice was associated with a differential response to injury by Schwann cells, by determining the percentage of proliferating and apoptotic cells in the nerve 5 d after crush. No differences in the number of BrdU-labeled cells were found between WT and TTR KO littermates (data not shown). Also, no differential cell survival was observed, as no differences were found between strains when the percentage of apoptotic cells was determined (data not shown). As no significant differences were found in the survival of either neurons or Schwann cells that could underlie the regeneration impairment in the absence of TTR, the persistence of macrophages was addressed in the distal stumps of regenerating nerves from WT and TTR KO mice 15, 30, and 75 d after nerve crush. Recruitment of macrophages is essential for rapid myelin clearance and therefore for regeneration to occur (Hirata and Kawabuchi, 2002); macrophages infiltrate the lesion site within 2 d and spread into the entire distal

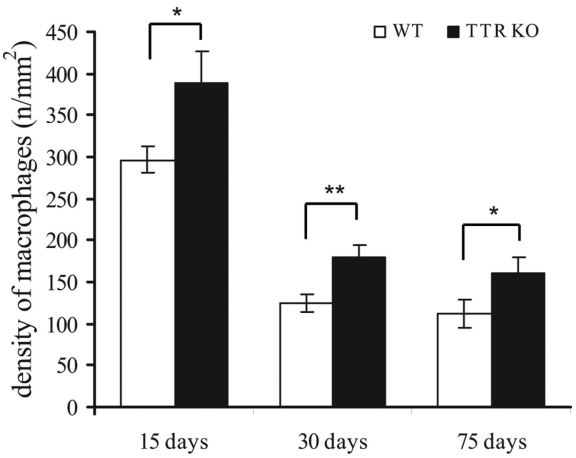

Figure 3. Macrophage response after nerve injury. Density of macrophages in regenerating nerves from WT and TTR KO mice 15, 30, and 75 d after nerve crush; $*p < 0.05$, $**p < 0.01$.

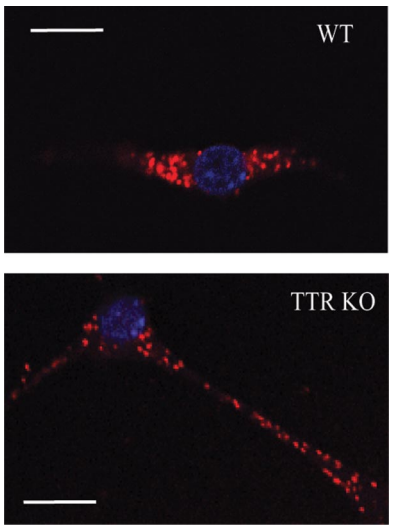

Figure 4. Retrograde transport in the presence and absence of TTR. Confocal images of WT and TTR KO DRG neurons 27 h after exposure to Tf-TR: in blue, DAPI staining, and in red, Tf-TR labeling. Scale bars, 10 μm.

stump after day 4 (Perry et al., 1987). At later time points, an increased macrophage number is recognized as an indicator that regeneration is compromised, as has been shown in other models of delayed axonal regeneration (Triolo et al., 2006). In both strains, as expected, the number of macrophages diminished with increased time of recovery (Fig. 3). Moreover, TTR KO mice presented a 30% increase in the density of macrophages after 15 d of regeneration, when compared with WT littermates; 30 and 75 d after nerve crush, this difference reached 45%. Such a persistence of macrophages in latter time points of regeneration is an additional indicator that myelin debris still exist in the nerves, i.e., that regeneration is delayed in TTR KO mice.

TTR KO mice present a compromised retrograde transport

To further understand the reason for the delayed regeneration in TTR KO mice, the capacity of WT and TTR KO axons to perform retrograde transport was assessed. In the case of impaired retrograde transport, the transmission of signals from the injury site to the cell body, that would allow the regrowth of fibers, might be compromised. $p75^{NTR}$ is a receptor that, upon binding to neurotrophins at axonal terminals, undergoes retrograde transport along the axon to the cell body (Curtis et al., 1995). Previous studies have shown that ligated nerves accumulate $p75^{NTR}$ in the distal side of the ligation, making this approach reliable for retrograde transport evaluation (Johnson et al., 1987, Taniuchi et al., 1988). Chronic constriction injury (CCI) was performed in WT ($n = 6$) and TTR KO ($n = 5$) mice and the accumulation of $p75^{NTR}$ in the distal side was determined 24 h after. TTR KO CCI nerves revealed a 26% decrease in the accumulation of $p75^{NTR}$ in the distal side of the ligation when compared with WT nerves ($p < 0.001$). To ensure that this decrease was not due to differential $p75^{NTR}$ expression, the levels of this protein were determined in WT and TTR KO intact nerves. No differences were observed between the two strains.

To further confirm that *in vivo* the absence of TTR is related to decreased levels of retrograde transport, WT ($n = 6$) and TTR KO ($n = 5$) sciatic nerves were retrogradely labeled with cholera toxin B. In agreement with the results obtained for the accumulation of $p75^{NTR}$, a decrease of ~30% was observed in the percentage of retrogradely labeled DRG neurons of TTR KO mice when compared with WT littermates ($p < 0.05$).

The relation between the absence of TTR and the lower levels of retrograde transport was additionally corroborated *in vitro*. For that, DRG neurons were cultivated and incubated with transferrin conjugated with Texas red (Tf-TR). Transferrin, a monomeric serum glycoprotein, binds iron for cell delivery through receptor-mediated endocytosis (Dautry-Varsat, 1986). When conjugated to Texas Red, transferrin functions as a tracer for retrograde transport (Liu et al., 2003). Twenty-seven hours after incubation, Tf-TR was only found in close proximity to the cell body in most WT DRG neurons (Fig. 4, top), while in the majority of TTR KO cells a more diffused labeling was found as Tf-TR was still present along neurites (Fig. 4, bottom). These differences in staining pattern are indicative of a slower retrograde transport in TTR KO DRG neurons. In fact, after quantification of the presence of Tf-TR in neurites and cell bodies, we determined that TTR KO DRG neurons presented a 20% decrease in the amount of retrogradely transported Tf-TR ($p < 0.001$). These *in vitro* findings correlate with the decreased accumulation of $p75^{NTR}$ in the distal portion of ligated TTR KO nerves, as well as with the decreased number of retrogradely labeled DRG neurons of TTR KO mice found *in vivo*, and suggest that lack of TTR is associated not only with decreased neurite outgrowth, but also with impaired retrograde transport.

In vitro, TTR is internalized by neurons through a clathrin-dependent mechanism

Since, *in vitro*, neurite outgrowth is increased by the presence of TTR (Fleming et al., 2007), we aimed at understanding how TTR action is exerted. For that, primary cultures of DRG neurons were incubated with hTTR-Alexa 488 for 3 h at 37°C. Confocal images along the *z*-axis showed that hTTR-Alexa 488 (in green) was internalized by DRG neurons. For visualization of cell bodies and neurites, the neuron specific protein PGP 9.5 (in red) was used. hTTR-Alexa 488 was prominently found in neurites (Fig. 5*A*, top panels, highlighted by arrows) but was also found within cell bodies (Fig. 5*A*, bottom panels, highlighted by arrows). Moreover, TTR internalization presented a punctate-like pattern (Fig. 5*A*), compatible with its presence within vesicles.

To establish whether TTR internalization was receptor-mediated, DRG neurons were incubated with hTTR-Alexa 488 for 3 h at 4°C, as at this temperature receptor-mediated endocytosis is inhibited. TTR internalization did not occur at 4°C, as

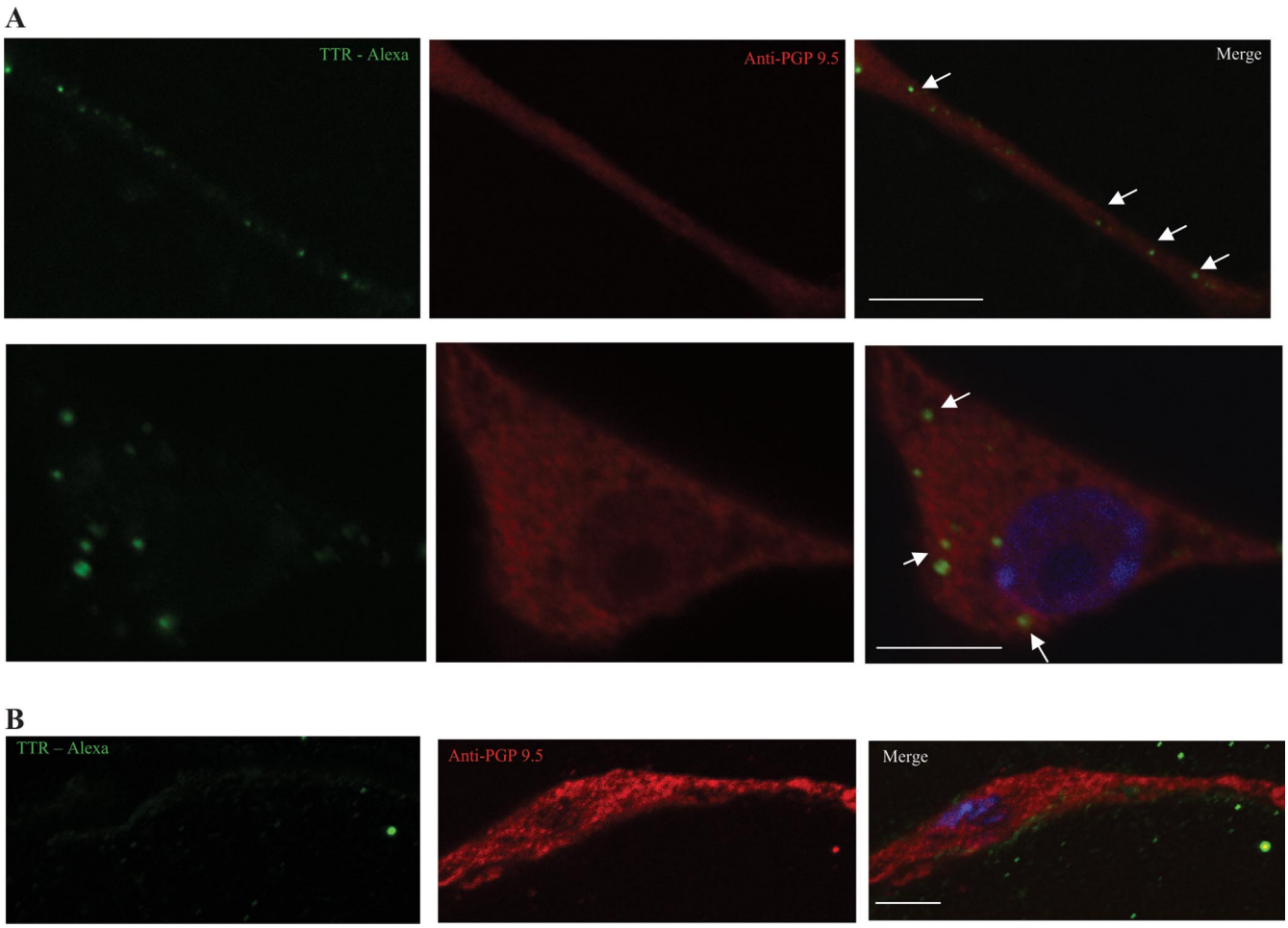

Figure 5. TTR internalization by DRG neurons. ***A***, ***B***, Confocal images of DRG neurons incubated with hTTR-Alexa 488 (in green) at 37°C (***A***, top shows a neurite and bottom shows a cell body) and at 4°C (***B***); anti-PGP 9.5 in red; internalized TTR highlighted by arrows. Scale bars, 10 μm.

hTTR-Alexa 488 was never found within DRG neurites or cell bodies (Fig. 5*B*), suggesting that TTR entry in neurons occurs through receptor-mediated endocytosis.

To further understand the mechanism through which TTR enters neurons, DRG neuron cultures were coincubated with hTTR-Alexa 488 and Tf-TR (in red), as transferrin endocytosis is known to be clathrin-dependent (Booth and Wilson, 1981). As shown in Figure 6*A*, hTTR-Alexa 488 vesicles partially colocalize with Tf-TR vesicles, suggesting that TTR endocytosis is clathrin-dependent. Reinforcing this finding, TTR did not colocalize with lipid rafts as shown by CT-B staining (in red) (Fig. 6*B*). In clathrin-coated pits, one of the major components, AP-2, is constitutively associated with Eps15, an accessory protein essential for early stages of clathrin-mediated endocytosis (Benmerah et al., 1998). To have additional proof that TTR endocytosis by DRG neurons is clathrin-dependent, GFP-tagged dominant negative constructs of Eps15 were transfected in DRG neurons. The two dominant-negative Eps15 mutants were: DIII and EΔ95/295 (Benmerah et al., 1998, 1999). As a control, DIIIΔ2 was used (Benmerah et al., 1998, 1999). The inhibition of transferrin uptake by both DIII and EΔ95/295 and the lack of effect of DIIIΔ2 are well described (Benmerah et al., 2000). Given its toxicity (A. Benmerah, personal communication), transfection of DRG neurons with the mutant EΔ95/295 resulted in high levels of cell death and as such only results obtained with the DIII dominant-negative Eps15 construct are described. In support of clathrin-mediated endocytosis, neurons transfected with the GFP-DIII construct displayed a reduced uptake of hTTR-Alexa 568 (Fig. 6*C*, top) when compared with DRG neurons transfected with the control construct GFP-DIIIΔ2 where TTR was taken up into the cytoplasm presenting the characteristic punctuate-like staining (Fig. 6*C*, bottom, arrowheads). Quantification of internalized hTTR-Alexa 568 using confocal images along the *z*-axis, revealed that in fact DRG neurons transfected with the GFP-DIII construct internalized 65% less hTTR-Alexa 568 than DRG neurons transfected with the control construct GFP-DIIIΔ2 ($p < 0.05$).

TTR internalization is required for neurite outgrowth enhancement

Similarly to DRG neurons, PC12 cells grown in the absence of TTR, i.e., with TTR KO serum, were previously shown to display a 30% decreased size of the longest neurite per cell, when compared with cells grown with WT serum (Fleming et al., 2007). Moreover, addition of TTR to TTR KO serum was able to rescue this phenotype. To understand whether TTR internalization is needed for the ability of TTR to enhance neurite outgrowth, additional experiments were performed where TTR KO serum was supplemented with TTR coupled to 1 μm-diameter polystyrene beads, FluoSpheres, which prevent TTR internalization due to their size. It is noteworthy that similar strategies using FluoSpheres were previously applied to address NGF internalization by neurons (Riccio et al., 1997; MacInnis and Campenot, 2002).

As a control, cells were also exposed to TTR KO serum supplemented with either FluoSpheres only or with FluoSpheres and free TTR. First, the efficacy of TTR binding to FluoSpheres was assessed: >90% of WT TTR was bound to the FluoSpheres and no detectable free TTR was found within the last wash (data not shown). Second, the biological activity of TTR coupled to FluoSpheres was assessed. TTR is a homotetrameric protein where the arrangement of the four subunits forms a central hydrophobic channel where T_4 binds (Blake et al., 1974). Given that the four TTR subunits need to be correctly structured so that T_4 binding is accomplished, this property of the protein was chosen to evaluate its structural integrity after conjugation to FluoSpheres. TTR coupled to FluoSpheres was efficient in binding T_4 (data not shown). As such, although it cannot be totally ruled out, it is unlikely that the results obtained with TTR conjugated to FluoSpheres might be the consequence of loss of function on sensory neurons caused by structural changes in the protein. Regarding neurite outgrowth, as previously described, absence of TTR in the cell culture medium (KO) was related to decreased size of the longest neurite, and addition of free TTR (KO + free TTR) was able to rescue this phenotype (Fig. 7). Addition of FluoSpheres to TTR KO serum did not alter neurite outgrowth (KO + FluoSpheres only). When PC12 cells were exposed to TTR KO serum supplemented with TTR coupled to FluoSpheres (KO + TTR coupled to FluoSpheres), neurite size was similar to the situation where cells were exposed to TTR KO serum alone (KO) (Fig. 7). Moreover, the addition of FluoSpheres and free TTR (KO + FluoSpheres + free TTR) rescued this phenotype, suggesting that the mechanism by which TTR enhances neurite outgrowth requires the internalization of the protein. To ascertain that the phenotype found was due to the inhibition of TTR internalization and not to the inactivation of specific residues of the protein, amine- and carboxylate-modified FluoSpheres were used in these assays. The results obtained were equivalent and independent of the type of FluoSpheres used (data not shown). This experiment was performed using PC12 cells as DRG neurons revealed to be sensitive to FluoSpheres which, under the conditions used, lead to the inhibition of neurite outgrowth independently of protein coupling.

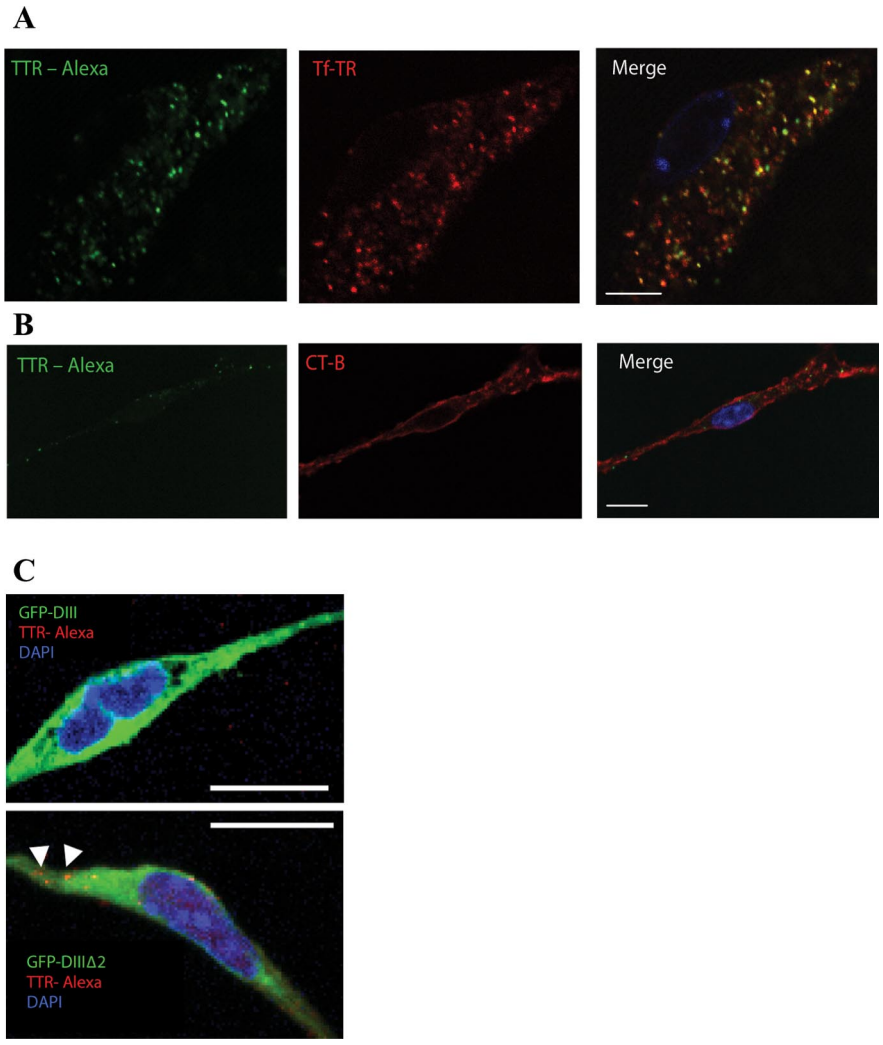

Figure 6. TTR internalization by DRG neurons is clathrin mediated. ***A***, Coincubation of DRG neurons with hTTR-Alexa 488 (green) and Tf-TR (red). ***B***, Coincubation of DRG neurons with hTTR-Alexa 488 (green) and CT-B (red). Scale bar, 10 μm. ***C***, *z*-axis stacking of hTTR-568 (red) uptake by DRG neurons transfected with either GFP-tagged DIII (green) (top) or DIIIΔ2 constructs (green) (bottom); DAPI staining in blue. Scale bar, 10 μm.

Megalin is expressed by DRG neurons and is necessary for TTR neuritogenic effect

Given that one endocytic TTR receptor, megalin, has been identified, being important for preventing TTR filtration through the glomerulus (Sousa et al., 2000) and since megalin was recently implicated in metallothionein uptake by neurons (Fitzgerald et al., 2007; Ambjørn et al., 2008), we hypothesized that megalin might be involved in the uptake of TTR. To verify whether DRG neurons express megalin, RT-PCR and immunohistochemistry were performed. Kidney was used as a positive control since megalin is abundantly expressed in this organ. As shown in Figure 8*A* and *B*, both methodologies demonstrate that megalin is expressed in DRG neurons. To demonstrate that a sheep anti-rat megalin antibody blocks TTR entrance in DRG neurons, similarly to what has been previously demonstrated for metallothionein uptake by kidney cells (Klassen et al., 2004), we performed the analysis of hTTR-Alexa 488 uptake in DRG neurons incubated with either nonimmune sheep serum or sheep anti-rat megalin. DRG neurons treated with the anti-megalin antibody (Fig. 8*C*, right) displayed less hTTR-Alexa 488 internalized when compared with DRG neurons incubated with nonimmune sheep serum (Fig. 8*C*, left). Quantification of internalized hTTR-Alexa 488 using confocal images along the *z*-axis, showed that DRG neurons where megalin was functionally blocked by the anti-megalin antibody revealed ~50% decreased hTTR-Alexa 488 entry relatively to DRG neurons incubated with nonimmune sheep serum ($p < 0.05$), similarly to what has previously been demonstrated for TTR uptake by kidney cells (Sousa et al., 2000). In light of these results, neurite outgrowth induced by TTR was measured after megalin blocking by anti-megalin. As previously described (Fleming et al., 2007), TTR KO DRG neurons grown in the pres-

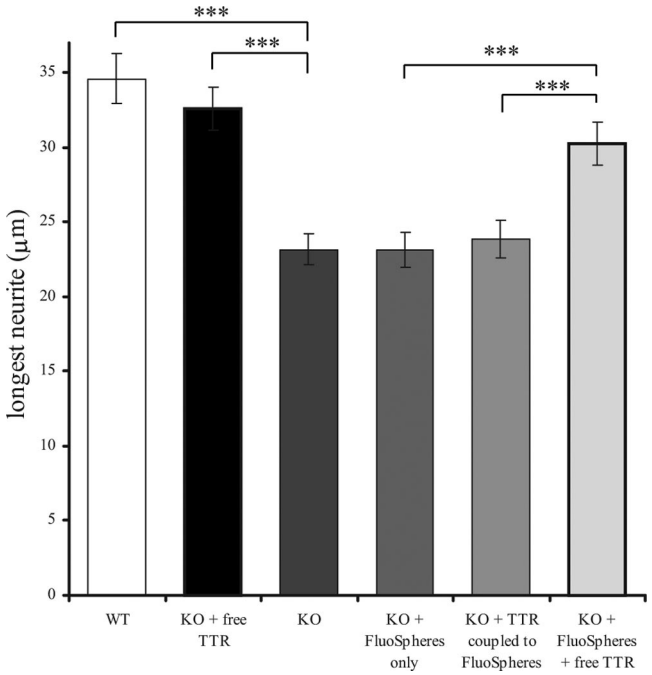

Figure 7. Neurite outgrowth in the presence of FluoSpheres. Average size of the longest neurite of PC12 cells after exposure to WT serum (WT), or to TTR KO serum alone (KO), or supplemented with either free TTR (KO + free TTR), FluoSpheres (KO + FluoSpheres only), TTR coupled to FluoSpheres (KO + TTR coupled to FluoSpheres), or FluoSpheres and free TTR (KO + FluoSpheres + free TTR). ***$p < 0.001$.

ence of TTR (+TTR) presented increased size of the longest neurite when compared with cells grown in TTR-free medium (Fig. 8*D*). TTR action was not affected by the addition of IgG (+TTR + IgG) (Fig. 8*D*). However, when DRG neurons were coincubated with TTR and anti-megalin (+TTR + α megalin), TTR enhancement of neurite size was no longer observed (Fig. 8*D*), showing that TTR internalization by neurons, which is needed for the protein to exert its neuritogenic activity, is megalin-dependent. As a control, the anti-megalin antibody was added to the culture medium (+ α megalin) and no difference was observed relatively to cells grown with culture medium alone. As an additional control, sheep serum was added to TTR KO DRG neurons, and again no difference was found when compared with cells grown with culture medium alone.

In vivo, decreased megalin leads to decreased nerve regeneration and its action is TTR-dependent

To assess the influence of megalin in the action of TTR *in vivo*, nerve crush of WT, TTR KO, megalin heterozygous (MEG (+/−)) and TTR KO/MEG (+/−) animals was done and mice were allowed to recover for 15 d. This experiment was performed with megalin heterozygous instead of megalin KO mice as most of the latter animals die within minutes after birth (Willnow et al., 1996). We started by determining that MEG (+/−) mice expressed ~50% less megalin in the DRG when compared with WT littermates (Fig. 9*A*) ($p < 0.05$). MEG (+/−) mice, producing a reduced amount of the receptor in the DRG, presented a 28% decrease in the density of myelinated fibers 15 d after crush when compared with WT animals (Fig. 9*B*). As previously described (Fleming et al., 2007), TTR KO mice also presented a 30% decrease in the density of myelinated fibers (Fig. 9*B*), emphasizing the role of TTR in nerve regeneration, and suggesting that in the absence of TTR, other megalin ligands have no influence in the progression of regeneration in the sciatic nerve. These findings additionally suggest that megalin is an important player in the course of nerve regeneration as its partial absence is sufficient to impair TTR-mediated enhancement of this process. Supporting this hypothesis, TTR KO/MEG (+/−) animals presented a similar regeneration impairment to both TTR KO and MEG (+/−) mice (Fig. 9*B*).

Discussion

In the present work we describe the mechanism of TTR action in neurons by showing that its neuritogenic effect is dependent on megalin-mediated internalization. We previously demonstrated that TTR enhances and accelerates regeneration (Fleming et al., 2007): 15 d after injury, the total number of myelinated fibers is 20% decreased in TTR KO mice (reaching WT levels after 30 d of regeneration), whereas in the case of unmyelinated fibers, differences are observed later, at 30 d after injury, when mice lacking TTR show a 40% decrease. More importantly, these differences have consequences at the functional level as TTR KO mice present a decreased locomotor activity and motor nerve conduction velocity throughout regeneration, clearly demonstrating that TTR enhances and accelerates this process. Such an effect is relevant in the scenario of nerve regeneration as timely target innervation is crucial for regain of functional capacity. Here, the impact of TTR in nerve regeneration was further established through the demonstration that local TTR delivery was successful in abolishing the differences between WT and TTR KO mice. Regarding the cellular response to nerve injury, TTR KO mice present no significant differences in both Schwann cell proliferation and survival when compared with WT littermates, suggesting that these mechanisms are not responsible for their delayed regeneration. Moreover, after nerve crush, no differences in the g ratio between strains were reported (Fleming et al., 2007), ruling out an impairment in myelination. The fact that TTR KO mice present an increased number of macrophages in the nerve after injury is probably an indicator that regeneration is compromised and that the removal of debris is delayed. Regarding the neuronal response to injury, the absence of TTR is not related to increased neuronal death after nerve crush that could underlie the diminished number of axons undergoing regeneration, but is instead related to delayed axonal growth (Fleming et al., 2007). Additionally to a decreased axonal growth, our present results demonstrate that TTR KO axons have lower levels of retrograde transport both *in vitro* and *in vivo*. Being the transmission of signals to the cell body a key process in nerve regeneration, the compromised retrograde transport of TTR KO axons might be, at least in part, responsible for the delayed regenerative capacity of TTR KO mice and decreased neurite outgrowth in the absence of TTR.

Our results show additionally that WT TTR is readily detectable within the peripheral nerve which is in agreement with the previous demonstration of TTR presence in the endoneurial fluid of human and rat nerves (Saraiva et al., 1988). The fact that TTR is present in the nerve under physiological conditions, as is here shown, further elucidates why, when mutated, TTR preferentially deposits in FAP peripheral nerves. In recipients of FAP livers, TTR deposits were found within the nerve, suggesting that plasma TTR can cross the BNB (M. M. Sousa et al., 2004). Our studies using intravenous injection of hTTR-Alexa 488 show that plasma TTR is in fact able to enter intact nerves through the BNB, which is effective in slowing but not in preventing the entry of proteins into the endoneurium (Wadhwani and Rapoport, 1994). This is in agreement with previous studies showing that intravenously injected albumin was conspicuously found

throughout nerve connective tissue and in basement membranes surrounding nerve fibers (Allen and Kiernan, 1994), similarly to what we here show for TTR. On the other hand, when an injury takes place, plasma TTR has its entrance in the nervous tissue facilitated, as the BNB is disrupted. In summary, our data further substantiates that *in vivo* TTR is present in the nerve and, as such, is able to contribute to the enhancement of nerve regeneration and neurite outgrowth in the settings of nerve injury.

In vitro, DRG neurons were able to internalize TTR by a clathrin-dependent endocytic process. The biological significance of TTR internalization was confirmed by the fact that the enhancement of neurite outgrowth by TTR was only possible when free TTR was used, being abolished when the protein was prevented from being internalized. Two endocytic TTR-related receptors have been described, namely megalin (Sousa et al., 2000) and an unidentified receptor-associated protein (RAP)-sensitive receptor (Sousa and Saraiva, 2001). Megalin, a member of the LDL receptor family, is involved in receptor-mediated endocytosis in clathrin-coated pits of a wide range of ligands, such as albumin (Zhai et al., 2000), and was described as being important for preventing TTR filtration through the glomerulus (Sousa et al., 2000). Later, it was shown that TTR internalization by liver cells is associated to lipoprotein metabolism, and that an unidentified RAP-sensitive receptor mediates TTR uptake (Sousa and Saraiva, 2001). Regarding the nervous system, megalin has been described as an important protein for the development of the forebrain (Willnow et al., 1996; Spoelgen et al., 2005) and spinal cord (Wicher and Aldskogius, 2008). Furthermore, megalin was thought to be expressed exclusively by epithelial cells; however, very recently, several reports have shown that megalin is expressed by other cell types, namely oligodendrocytes (Wicher et al., 2006), astrocytes (Bento-Abreu et al., 2008), and neurons, including retinal ganglion cells (Fitzgerald et al., 2007), cortical neurons (Chung et al., 2008), and cerebellar granule neurons (Ambjørn et al., 2008). We now show that DRG neurons also express megalin and that TTR neuritogenic activity depends on its internalization by this receptor. Interestingly, it was recently reported that metallothionein stimulation of neurite outgrowth in retinal ganglion cells (Fitzgerald et al., 2007) and cerebellar granule neurons (Ambjørn et al., 2008) is mediated by megalin. Considering that TTR interacts with metallothionein (Gonçalves et al., 2008) and that the present work demonstrates that TTR neuritogenic effect is megalin dependent, the relationship between these molecules and neurite outgrowth should be further studied. The present work also reveals that, *in vivo*, decreased levels of megalin lead to decreased nerve regeneration, further substantiating the importance of this receptor in the nervous system and particularly in the course of nerve regeneration. Although MEG (+/−) mutants are generally described as lacking a major phenotype, a semidominant effect through haplo-insufficiency resulting in decreased levels of megalin has been shown to cause progressive hearing loss in these animals (König et al., 2008). In support of diminished levels of megalin in MEG (+/−) mice, these were shown to present transferrin excretion in the urine, in contrast to WT mice (Kozyraki et al., 2001). Here we show that similarly to the latter tissues, MEG (+/−) DRG have a decreased expression of the receptor when compared with WT littermates. The importance of megalin in the nerve is supported by the fact that its partial absence is sufficient to impair TTR-mediated enhancement of nerve regeneration. Our data additionally suggests that, in the case of sciatic nerve regeneration, other megalin ligands have no influence, as TTR KO mice have a similar decrease in nerve regeneration as MEG (+/−) mice. This further suggests that megalin and TTR may act in the same pathway. It is worth mentioning that it is possible that additionally, TTR may generate its effect via signal transduction pathways ac-

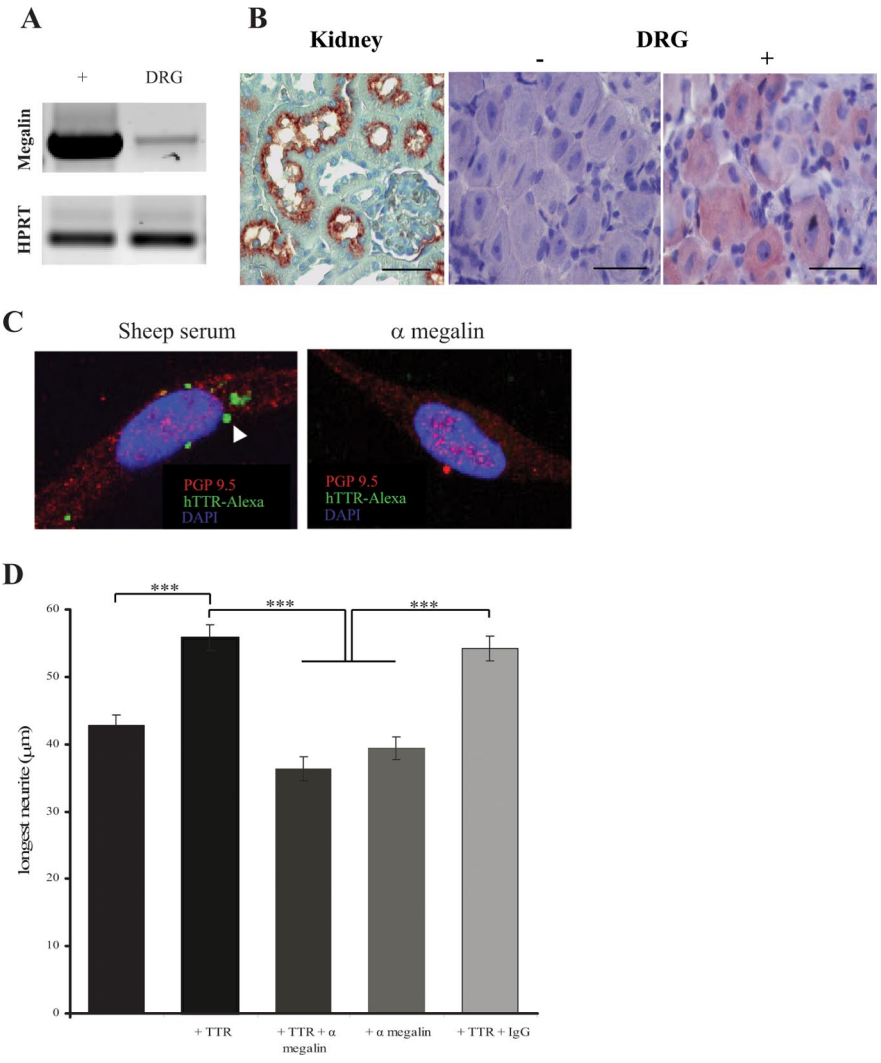

Figure 8. TTR internalization by DRG neurons is megalin mediated. ***A***, Megalin and HPRT RT-PCR of kidney (+) and DRG. ***B***, Megalin immunohistochemistry of kidney (left), and DRG in the absence (−, middle) and presence (+, right) of primary antibody. Scale bar, 5 μm. ***C***, *z*-axis stacking of hTTR-Alexa 488 (green) uptake by DRG neurons preincubated with either nonimmune sheep serum (sheep serum, left) or sheep anti-rat megalin (α megalin, right); red: anti PGP 9.5 staining, blue: DAPI. ***D***, Average size of the longest neurite of TTR KO DRG neurons cells after exposure to B27 or B27 supplemented with TTR (+TTR), with TTR and anti-megalin (+TTR + α megalin), with anti-megalin (+α megalin), or with TTR and IgG (+TTR + IgG). ***$p < 0.001$.

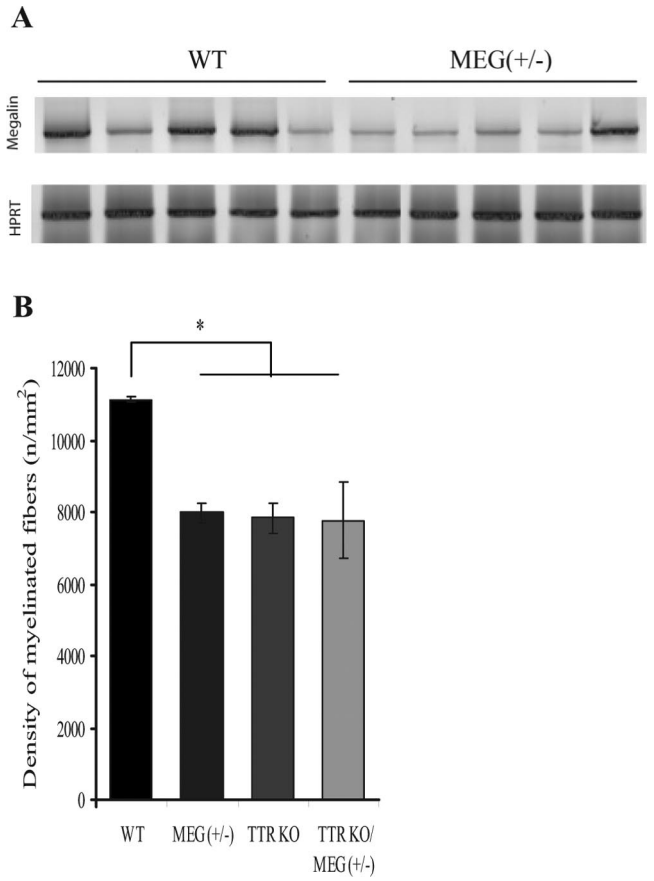

Figure 9. Decreased megalin levels lead to decreased nerve regeneration. ***A***, RT-PCR analysis of megalin and HPRT expression in MEG(+/−) and WT mouse DRG. ***B***, Morphometric analysis of sciatic nerves from WT, TTR KO, MEG(+/−), and TTR KO/MEG(+/−) mice. Density of myelinated fibers 15 d after nerve crush. *$p < 0.05$.

tivated by the NpxY motifs of the cytoplasmic tail of megalin, which interact with signaling molecules involved in the regulation of endocytosis (Qiu et al., 2006). It is also noteworthy that megalin is part of a ligand-dependent signaling pathway by enzymatic processing, linking receptor-mediated endocytosis with cell signaling (Zou et al., 2004).

In conclusion, our work further establishes the mechanism of TTR action in the nerve by showing that it has a direct effect on neurons, as its absence leads to impaired retrograde transport and decreased axonal growth. Also, we show that TTR effect in neurite outgrowth and nerve regeneration is mediated by megalin-dependent internalization. Finally, the relevance of TTR presence in the nerve may underlie its preferential deposition, when mutated, in the PNS of FAP patients.

References

Allen DT, Kiernan JA (1994) Permeation of proteins from the blood into peripheral nerves and ganglia. Neuroscience 59:755–764.

Ambjørn M, Asmussen JW, Lindstam M, Gotfryd K, Jacobsen C, Kiselyov VV, Moestrup SK, Penkowa M, Bock E, Berezin V (2008) Metallothionein and a peptide modeled after metallothionein, EmtinB, induce neuronal differentiation and survival through binding to receptors of the low-density lipoprotein receptor family. J Neurochem 104:21–37.

Andrade C (1952) A peculiar form of peripheral neuropathy. Familial atypical generalized amyloidosis with special involvement of the peripheral nerves. Brain 75:408–427.

Benmerah A, Lamaze C, Bègue B, Schmid SL, Dautry-Varsat A, Cerf-Bensussan N (1998) AP-2/Eps15 interaction is required for receptor-mediated endocytosis. J Cell Biol 140:1055–1062.

Benmerah A, Bayrou M, Cerf-Bensussan N, Dautry-Varsat A (1999) Inhibition of clathrin-coated pit assembly by an Eps15 mutant. J Cell Sci 112:1303–1311.

Benmerah A, Poupon V, Cerf-Bensussan N, Dautry-Varsat A (2000) Mapping of Eps15 domains involved in its targeting to clathrin-coated pits. J Biol Chem 275:3288–3295.

Bento-Abreu A, Velasco A, Polo-Hernández E, Pérez-Reyes PL, Tabernero A, Medina JM (2008) Megalin is a receptor for albumin in astrocytes and is required for the synthesis of the neurotrophic factor oleic acid. J Neurochem 106:1149–1159.

Blake CC, Geisow MJ, Swan ID, Rerat C, Rerat B (1974) Structure of human plasma prealbumin at 2–5 A resolution. A preliminary report on the polypeptide chain conformation, quaternary structure and thyroxine binding. J Mol Biol 88:1–12.

Booth AG, Wilson MJ (1981) Human placental coated vesicles contain receptor-bound transferrin. Biochem J 196:355–362.

Brouillette J, Quirion R (2008) Transthyretin: a key gene involved in the maintenance of memory capacities during aging. Neurobiol Aging 29:1721–1732.

Cheng C, Zochodne DW (2002) In vivo proliferation, migration and phenotypic changes of Schwann cells in the presence of myelinated fibers. Neuroscience 115:321–329.

Chung RS, Penkowa M, Dittmann J, King CE, Bartlett C, Asmussen JW, Hidalgo J, Carrasco J, Leung YK, Walker AK, Fung SJ, Dunlop SA, Fitzgerald M, Beazley LD, Chuah MI, Vickers JC, West AK (2008) Redefining the role of metallothionein within the injured brain: extracellular metallothioneins play an important role in the astrocyte-neuron response to injury. J Biol Chem 283:15349–15358.

Curtis R, Adryan KM, Stark JL, Park JS, Compton DL, Weskamp G, Huber LJ, Chao MV, Jaenisch R, Lee K (1995) Differential role of the low affinity neurotrophin receptor (p75) in retrograde axonal transport of the neurotrophins. Neuron 14:1201–1211.

Dautry-Varsat A (1986) Receptor-mediated endocytosis: the intracellular journey of transferrin and its receptor. Biochimie 68:375–381.

Episkopou V, Maeda S, Nishiguchi S, Shimada K, Gaitanaris GA, Gottesman ME, Robertson EJ (1993) Disruption of the transthyretin gene results in mice with depressed levels of plasma retinol and thyroid hormone. Proc Natl Acad Sci U S A 90:2375–2379.

Fitzgerald M, Nairn P, Bartlett CA, Chung RS, West AK, Beazley LD (2007) Metallothionein-IIA promotes neurite growth via the megalin receptor. Exp Brain Res 183:171–180.

Fleming CE, Saraiva MJ, Sousa MM (2007) Transthyretin enhances nerve regeneration. J Neurochem 103:831–839.

Gonçalves I, Quintela T, Baltazar G, Almeida MR, Saraiva MJ, Santos CR (2008) Transthyretin interacts with metallothionein 2. Biochemistry 47:2244–2251.

Hirata K, Kawabuchi M (2002) Myelin phagocytosis by macrophages and nonmacrophages during wallerian degeneration. Microsc Res Tech 57:541–547.

Johnson EM Jr, Taniuchi M, Clark HB, Springer JE, Koh S, Tayrien MW, Loy R (1987) Demonstration of the retrograde transport of nerve growth factor receptor in the peripheral and central nervous system. J Neurosci 7:923–929.

Klassen RB, Crenshaw K, Kozyraki R, Verroust PJ, Tio L, Atrian S, Allen PL, Hammond TG (2004) Megalin mediates renal uptake of heavy metal metallothionein complexes. Am J Physiol Renal Physiol 287:F393–F403.

König O, Rüttiger L, Müller M, Zimmermann U, Erdmann B, Kalbacher H, Gross M, Knipper M (2008) Estrogen and the inner ear: megalin knockout mice suffer progressive hearing loss. FASEB J 22:410–417.

Kozyraki R, Fyfe J, Verroust PJ, Jacobsen C, Dautry-Varsat A, Gburek J, Willnow TE, Christensen EI, Moestrup SK (2001) Megalin-dependent cubilin-mediated endocytosis is a major pathway for the apical uptake of transferrin in polarized epithelia. Proc Natl Acad Sci U S A 98:12491–12496.

Lindsay RM (1988) Nerve growth factors (NGF, BDNF) enhance axonal regeneration but are not required for survival of adult sensory neurons. J Neurosci 8:2394–2405.

Liu JJ, Ding J, Kowal AS, Nardine T, Allen E, Delcroix JD, Wu C, Mobley W, Fuchs E, Yang Y (2003) BPAG1n4 is essential for retrograde axonal transport in sensory neurons. J Cell Biol 163:223–229.

Liz MA, Faro CJ, Saraiva MJ, Sousa MM (2004) Transthyretin, a new cryptic protease. J Biol Chem 279:21431–21438.

MacInnis BL, Campenot RB (2002) Retrograde support of neuronal survival without retrograde transport of nerve growth factor. Science 295:1536–1539.

Madison R, da Silva CF, Dikkes P, Chiu TH, Sidman RL (1985) Increased rate of peripheral nerve regeneration using bioresorbable nerve guides and a laminin-containing gel. Exp Neurol 88:767–772.

Murakami T, Ohsawa Y, Sunada Y (2008) The transthyretin gene is expressed in human and rodent dorsal root ganglia. Neurosci Lett 436:335–339.

Nunes AF, Saraiva MJ, Sousa MM (2006) Transthyretin knockouts are a new mouse model for increased neuropeptide Y. FASEB J 20:166–168.

Perry VH, Brown MC, Gordon S (1987) The macrophage response to central and peripheral nerve injury. A possible role for macrophages in regeneration. J Exp Med 165:1218–1223.

Qiu S, Korwek KM, Weeber EJ (2006) A fresh look at an ancient receptor family: emerging roles for low density lipoprotein receptors in synaptic plasticity and memory formation. Neurobiol Learn Mem 85:16–29.

Riccio A, Pierchala BA, Ciarallo CL, Ginty DD (1997) An NGF-TrkA-mediated retrograde signal to transcription factor CREB in sympathetic neurons. Science 277:1097–1100.

Saraiva MJ (2001) Transthyretin mutations in hyperthyroxinemia and amyloid diseases. Hum Mutat 17:493–503.

Saraiva MJ, Makover A, Moriwaki H, Blaner W, Costa PP, Goodman DS (1988) Studies on transthyretin metabolism in the nervous system. In: Amyloid and smyloidosis (Isobe T, Araki S, Uchino F, Kito S, Tsubura E, eds), pp 343–348. New York: Plenum.

Sousa JC, Grandela C, Fernández-Ruiz J, de Miguel R, de Sousa L, Magalhães AI, Saraiva MJ, Sousa N, Palha JA (2004) Transthyretin is involved in depression-like behaviour and exploratory activity. J Neurochem 88:1052–1058.

Sousa MM, Saraiva MJ (2001) Internalization of transthyretin. Evidence of a novel yet unidentified receptor associated protein (RAP)-sensitive receptor. J Biol Chem 276:14420–14425.

Sousa MM, Saraiva MJ (2003) Neurodegeneration in familial amyloid polyneuropathy: from pathology to molecular signalling. Prog Neurobiol 71:385–400.

Sousa MM, Saraiva MJ (2008) Transthyretin is not expressed by dorsal root ganglia cells. Exp Neurol 214:362–365.

Sousa MM, Norden AG, Jacobsen C, Willnow TE, Christensen EI, Thakker RV, Verroust PJ, Moestrup SK, Saraiva MJ (2000) Evidence for the role of megalin in renal uptake of transthyretin. J Biol Chem 275:38176–38181.

Sousa MM, Ferrão J, Fernandes R, Guimarães A, Geraldes JB, Perdigoto R, Tomé L, Mota O, Negrão L, Furtado AL, Saraiva MJ (2004) Deposition and passage of transthyretin through the blood-nerve barrier in recipients of familial amyloid polyneuropathy livers. Lab Invest 84:865–873.

Spoelgen R, Hammes A, Anzenberger U, Zechner D, Andersen OM, Jerchow B, Willnow TE (2005) LRP2/megalin is required for patterning of the ventral telencephalon. Development 132:405–414.

Taniuchi M, Clark HB, Schweitzer JB, Johnson EM Jr (1988) Expression of nerve growth factor receptors by Schwann cells of axotomized peripheral nerves: ultrastructural location, suppression by axonal contact, and binding properties. J Neurosci 8:664–681.

Triolo D, Dina G, Lorenzetti I, Malaguti M, Morana P, Del Carro U, Comi G, Messing A, Quattrini A, Previtali SC (2006) Loss of glial fibrillary acidic protein (GFAP) impairs Schwann cell proliferation and delays nerve regeneration after damage. J Cell Sci 119:3981–3993.

Wadhwani KC, Rapoport SI (1994) Transport properties of vertebrate blood-nerve barrier: comparison with blood–brain barrier. Prog Neurobiol 43:235–279.

Wicher G, Aldskogius H (2008) Megalin deficiency induces critical changes in mouse spinal cord development. Neuroreport 19:559–563.

Wicher G, Larsson M, Svenningsen AF, Gyllencreutz E, Rask L, Aldskogius H (2006) Low density lipoprotein receptor-related protein-2/megalin is expressed in oligodendrocytes in the mouse spinal cord white matter. J Neurosci Res 83:864–873.

Willnow TE, Hilpert J, Armstrong SA, Rohlmann A, Hammer RE, Burns DK, Herz J (1996) Defective forebrain development in mice lacking gp330/megalin. Proc Natl Acad Sci U S A 93:8460–8464.

Zhai XY, Nielsen R, Birn H, Drumm K, Mildenberger S, Freudinger R, Moestrup SK, Verroust PJ, Christensen EI, Gekle M (2000) Cubilin- and megalin-mediated uptake of albumin in cultured proximal tubule cells of opossum kidney. Kidney Int 58:1523–1533.

Zou Z, Chung B, Nguyen T, Mentone S, Thomson B, Biemesderfer D (2004) Linking receptor-mediated endocytosis and cell signaling: evidence for regulated intramembrane proteolysis of megalin in proximal tubule. J Biol Chem 279:34302–34310.